Measurement of Coherent Drift-Wave Ion-Fluid Velocity Field When Ion Dynamics Are Stochastic

A. D. Bailey III,* R. A. Stern,† and P. M. Bellan
California Institute of Technology, Pasadena, California 91125
(Received 4 February 1993)

In order to test the validity of the fluid drift approximation when ion dynamics are stochastic, the time-dependent ion-fluid velocity field in a coherent, drift-Alfvén wave has been measured in Caltech's Encore tokamak using plasma planar laser induced fluorescence. Many measured parameters of the wave are well described by the drift approximation above a threshold for stochastic ion dynamics, including the flow pattern in the single measured component of the ion-fluid velocity field. Surprisingly, the theory fails at a fundamental level by predicting flow speeds 10 times larger than those measured ($|u_{max}| \approx 10^5$ cm/s).

PACS numbers: 52.35.Kt, 52.70.Kz

The drift approximation describing the fluid behavior of ions and electrons is one of the most used and successful approximations in plasma physics. Since the two-fluid equations of motion are derived by integrating over particle distribution functions, the exact nature of the individual particle dynamics may be expected to play a minor role in plasma behavior that follows the fluid equations. Although stochastic dynamics are used to describe many plasma phenomena currently under study [1], there is no general theory predicting the consequences of stochastic dynamics on the validity range of the drift approximation in fluid plasma phenomena. We have studied the effects of stochastic ion dynamics in a coherent drift-Alfvén wave which has been well characterized using the fluid drift approximation in Caltech's Encore tokamak [2]. Recent measurements have shown that electrostatic waves in magnetized plasmas can cause ion orbits to become stochastic [3,4]. In our system, single point laser induced fluorescence (LIF) measurements have shown [4] that ion orbits become stochastic if the drift wave potential $\tilde{\phi}$ is large enough that the normalized drift wave amplitude α exceeds a threshold

$$\alpha = k^2\tilde{\phi}/\omega_{ci}B \gtrsim 1 ,$$

where k is the wave number, ω_{ci} is the ion cyclotron angular frequency, and B is the magnetic field. One observed manifestation of the transition to stochasticity is that the ion velocity distributions are hotter than predicted by standard heating mechanisms [4]. Even above the stochastic threshold we observe that the wave frequency, propagation vector, and phase relationship between the oscillating density and potential are still well described by the two-fluid model based on the drift approximation. This is an example of a fluid plasma phenomena where *many* measured parameters appear well characterized by the drift approximation ignoring particle stochasticity, but it is unclear if this is true for *all* plasma parameters. To further test the validity of the drift approximation in the presence of stochastic ion orbits, we have developed the first plasma *planar* laser induced fluorescence (PLIF) diagnostic to measure the time-resolved ion velocity field in a poloidal cross section of Encore. Surprisingly, we find that although the measured ion-fluid velocity flow *pattern* is well described by the drift approximation, the *magnitude* of the measured flow is an order of magnitude smaller than predicted. Besides highlighting the need for a self-consistent theory incorporating stochastic dynamics, this result shows that the drift approximation cannot be used confidently to calculate unmeasured plasma parameters in the presence of stochastic ion dynamics even when many measured parameters obey the drift approximation. This may have important implications for the calculated magnitude of the radial electric field in tokamaks during H-mode transition since the field strength is calculated using the drift approximation and measured ion velocity profiles [5].

The PLIF measurements reported in this Letter, the first ion-fluid velocity field measurements in *two* spatial dimensions, are compared with the prediction of the drift approximation calculated using Langmuir probe measurements of the plasma potential. This fundamental comparison between the measured ion velocity field and theoretical prediction has not previously been made due to the experimental difficulty in simultaneously measuring the ion velocity field and plasma potential with sufficient spatial and temporal resolution. Previous measurements of ion-fluid rotation velocities ($\gtrsim 10^5$ cm/s) have been made in spheromaks during formation [6] using the Doppler shifts of *spontaneously* emitted lines of impurity ions and in large tokamaks using charge exchange recombination spectroscopy [5]. Interpretation of raw data in Refs. [5,6] depended on plasma models of the emission profiles and Abel inversion of chord averaged measurements. The plasma potential in these plasmas was not directly measured. The scheme we are using, laser *induced* fluorescence (LIF), is a *directly interpreted* and *spatially localized* technique that gives precise ion velocity distributions. The LIF intensity measured while scanning the wavelength of a narrow linewidth laser through a resonant ion absorption line is proportional to the ion velocity distribution when Doppler broadening dominates the absorption linewidth. LIF has been used to obtain rotation profiles in a plasma column from the Doppler shifted peaks of majority ion velocity distribu-

0031-9007/93/71(19)/3123(4)$06.00

tions [7], and also to make detailed, time-resolved measurements of ion velocity distributions in *one* spatial dimension in driven electrostatic waves [8]. Although PLIF from neutral atoms has been used in fluid visualization [9], these are the first PLIF images from *plasma* ions, extending the capabilities of plasma LIF to two spatial dimensions.

Our experiments were conducted on Ar discharges in Caltech's high repetition rate Encore tokamak (major radius $R=38$ cm, minor radius $a=13$ cm, repetition rate=15 Hz, pulse length ≈ 1 ms). The plasma parameters are density $n \approx 10^{12}$ cm^{-3}, electron temperature $\langle T_e \rangle \approx 9$ eV, ion temperature $\langle T_i \rangle \approx 6$ eV, peak $T_i \approx 10$ eV, peak plasma current $I_p = 1.35$ kA, and on-axis toroidal magnetic field $B = 275$ G giving an ion cyclotron frequency $f_{ci} \approx 10$ kHz. These discharges have reproducible, coherent, current driven, nearly electrostatic drift-Alfvén waves with poloidal mode number $m=2$ and frequency $f \approx 5$ kHz which propagate in the electron diamagnetic direction as predicted by a theory using the drift approximation [2]. The Langmuir probe measured wave amplitude $\tilde{\phi}_p \approx 10$ V peak to peak gives a normalized wave amplitude $\alpha \approx 2$ well above the stochastic threshold as confirmed by the hot ion temperatures measured by PLIF.

Figure 1 shows the experimental setup. PLIF at 4610 Å from the Ar II transition $4p'^2F^0_{7/2} \rightarrow 4s'^2D_{5/2}$ is excited by a narrow linewidth ($\Delta f = 1.3$ GHz) YAG pumped dye laser in resonance with the Doppler broadened transition from the metastable $3d'^2G_{9/2} \rightarrow 4p'^2F^0_{7/2}$. The pulsed 6115 Å laser beam ($\Delta t \approx 15$ ns, $E \approx 300$ μJ/pulse) is expanded into a 0.5 mm×13 cm sheet by a cylindrical lens.

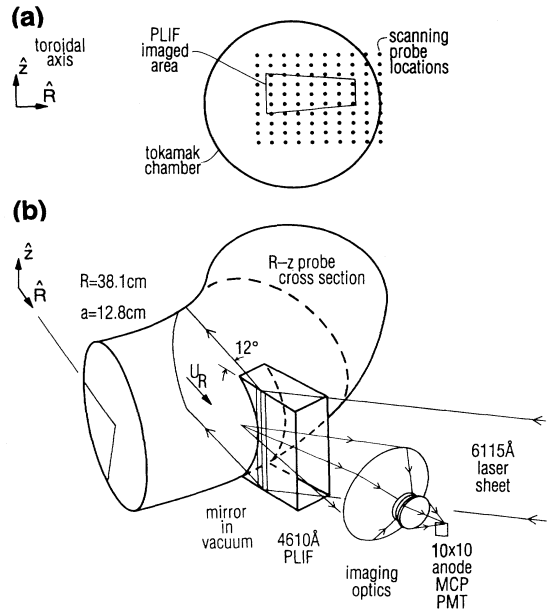

FIG. 1. (a) Positions of Langmuir probe measurements and projection of PLIF area in a poloidal cross section. (b) Experimental setup.

As shown in Fig. 1(b), the sheet enters the vacuum vessel through a large port window and is reflected across the chamber by a vertical mirror. A beam dump prevents scattered light from inducing fluorescence outside the laser sheet. Plasma radiation and PLIF excited in the nearly poloidal cross section exit through the same window. The light is filtered and imaged onto the photocathode of a gated, 10×10 anode, microchannel plate photomultiplier (Hamamatsu R3801). A low f number Fresnel lens collects the weak PLIF signal ($\sim 10^{-9}$ W/sr). All rays pass nearly paraxially through the narrow bandwidth (10 Å) interference filter sandwiched between a negative-positive lens pair. Since image magnification varies across the square anode array, the imaged plasma is trapezoidal [see Fig. 1(a)] and anode resolution varies from 9×4 mm^2 to 20×7 mm^2.

Figure 2 shows the coherent density oscillations of the wave measured with a Langmuir probe biased to collect the ion saturation current in the plasma edge. The waves in each discharge are reproducible so variable time delays from the tokamak trigger are used to trigger PLIF data acquisition in phase with the waves. During a PLIF experiment digitized signals proportional to the integrated current pulses from each PMT anode are saved using CAMAC controlled gated integrators (Transiac 7004 with 50-ns gate). At a given time in the discharge, ion velocity distributions are measured by scanning the dye laser wavelength and measuring the resulting PLIF intensity. These measurements were averaged over 75 discharges for each of 51 wavelengths ($\Delta\lambda = 0.01$ Å). Since the detected signal is the sum of the velocity-dependent PLIF and the velocity-independent spontaneous emission (2–5 times weaker), the data set for each anode is χ^2 fitted to a Maxwellian superimposed on a constant background. The ion fluid velocity parallel to the laser propagation vector is $u_R = c\Delta\lambda/\lambda_0$ where $\Delta\lambda$ is the Doppler induced shift of the center wavelength from the PLIF absorption wavelength $\lambda_0 = 6114.92$ Å [10] for a stationary ion. The maximum measured wavelength shifts $\Delta\lambda \sim 0.03$ Å correspond to velocities $u_R \sim 1.5\times10^5$ cm/s.

The time-dependent spatial structure of the u_R field in

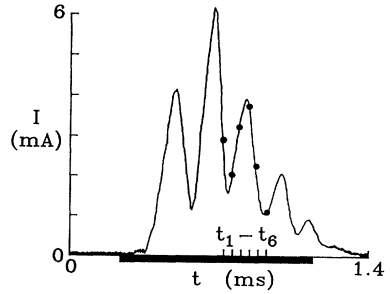

FIG. 2. Ion saturation current to a Langmuir probe showing coherent drift-Alfvén wave density fluctuations. Filled circles on trace mark the times ($\Delta t = 40$ μs) for data presented in Figs. 3 and 4. PLIF measurements were made at 20 μs intervals during the time indicated by the heavy bar on the time axis.

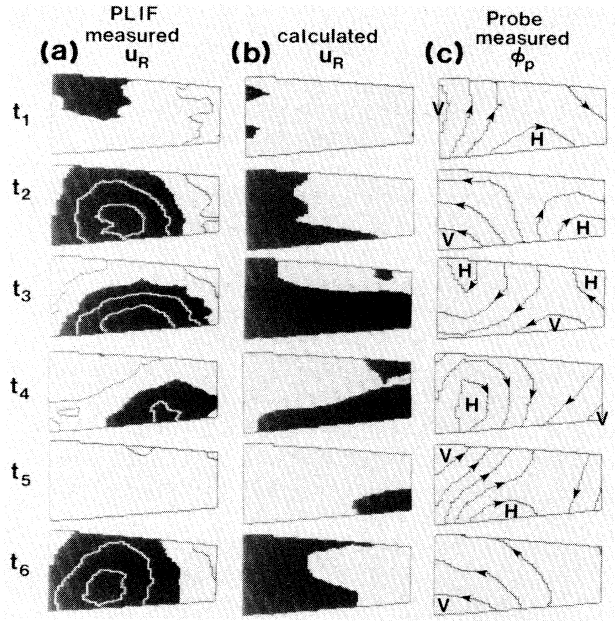

FIG. 3. (a) PLIF measured u_R field [full scale $\pm 1.1\times10^5$ cm/s, 2.8×10^4 (cm/s)/contour]. (b) u_R field calculated from probe and PLIF data in the drift approximation. Black (white) indicates u_R velocities to the left (right). (c) Langmuir probe measured $\tilde{\phi}_p$ (2 V/contour). Arrows on the equipotentials indicate the direction of $\mathbf{E}\times\mathbf{B}$ drifts around potential hills (H) and potential valleys (V). $\mathbf{B}$ points out of the page so that the electron diamagnetic rotation is counterclockwise. Times ($\Delta t = 40$ μs) correspond to those marked in Fig. 2. See Fig. 1 for correct spatial scales.

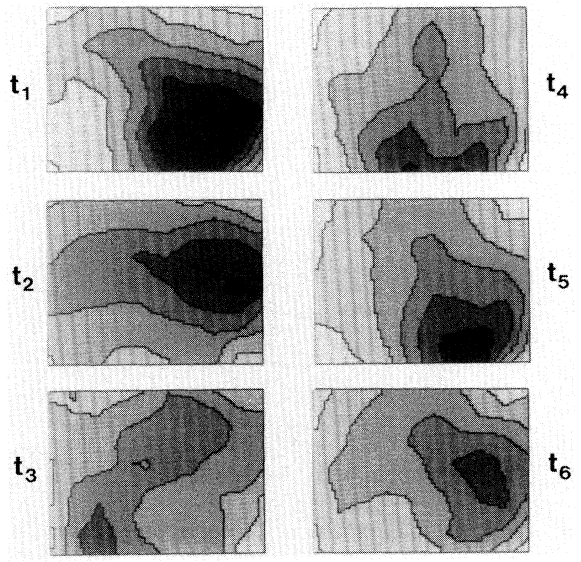

FIG. 4. Plasma density in a poloidal cross section showing dominant $m=2$ mode structure (peak density 3×10^{12} cm^{-3}, $\sim5\times10^{11}$ cm^{-3}/contour). $\mathbf{B}$ points out of the page so that the electron diamagnetic rotation is counterclockwise. Times ($\Delta t = 40$ μs) correspond to those marked in Fig. 2. See Fig. 1 for correct spatial scales.

the drift wave was measured using the PLIF diagnostic. The dominant feature of this structure is a periodic spatial rotation of localized regions of positive and negative u_R in phase with the wave. Six smoothed images of the u_R field at 40 μs intervals during a wave period are displayed in Fig. 3(a) (measurement times are shown in Fig. 2). Figure 3(a) shows that at t_1 the upper left corner of the imaged plasma has a negative u_R component. During the next 80 μs (t_2,t_3) the region moves down and to the right across the lower half of the image. The negative u_R region is shrinking into the lower right corner at t_4, disappearing altogether at t_5. A new region has dropped and expanded to fill the left half of the image to begin the cycle again at t_6. This pattern is observed for all five wave periods in this plasma and is typical of Encore discharges having coherent drift waves. Based on the consistency of many hundreds of measurements with repeatable spatial variations and the smooth variations in u_R observed on single anodes, the estimated uncertainty in the u_R measurements is $\pm 8\times10^3$ cm/s.

The two-dimensional flow field consistent with these data is not obvious since only the single component u_R is measured. To interpret the PLIF data in Fig. 3(a), Langmuir probe measurements were made in a nearby (separated toroidally by 0.1 parallel drift wavelengths) poloidal cross section as indicated in Fig. 1(b). Plasma I-V characteristics were measured by digitizing the current from the scanning probe biased to 12 voltages at each position [see Fig. 1(a)]. Using unmagnetized probe theory [11] the plasma potential ϕ_p, density, and T_e were determined. The density plots in Fig. 4 clearly show the dominance of the $m=2$ poloidal mode ($\tilde{n}/n \approx 0.5$) rotation in the electron diamagnetic direction. The mode structure is also apparent in the plasma potential ($\tilde{\phi}_p \approx 10$ V peak to peak) and electron temperature fluctuations ($\tilde{T}_e \approx 6$ eV peak to peak).

The ion fluid velocity perpendicular to the magnetic field in the drift approximation is the sum of the $\mathbf{E}\times\mathbf{B}$ and diamagnetic drifts so the $\hat{\mathbf{R}}$ component of the ion fluid velocity is

$$u_R = \hat{\mathbf{R}}\cdot\left[\frac{-\nabla\phi_p\times\mathbf{B}}{B^2} - \frac{\nabla(nT_i)\times\mathbf{B}}{enB^2}\right]. \quad (1)$$

Equation (1) together with the Langmuir probe data and the PLIF measured T_i allows us to calculate the theoretical prediction for u_R. Figure 3(b) shows u_R images *calculated* for the same sequence of times used in Fig. 3(a). Examination of Fig. 3(b) shows striking similarity between qualitative behavior of the negative u_R region in the calculated images and the PLIF measured images in Fig. 3(a).

The $\mathbf{E}\times\mathbf{B}$ drift is the dominant drift determining the direction of u_R. In a stationary two-dimensional potential, the $\mathbf{E}\times\mathbf{B}$ drift is along potential contours. With $\mathbf{B}$ out of the page the drift is counterclockwise around po-

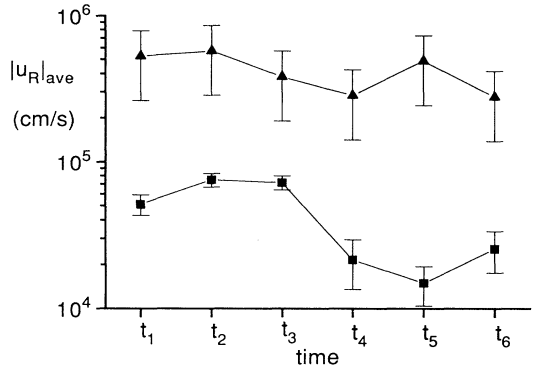

FIG. 5. Comparison of $|u_R|$ averaged over the imaged plasma as measured by PLIF (squares) and calculated using the drift approximation (triangles). Times ($\Delta t = 40$ μs) correspond to those marked in Fig. 2.

tential valleys and clockwise around potential hills. In Fig. 3(c) ϕ_p is displayed with arrows on the equipotentials to indicate the $\mathbf{E}\times\mathbf{B}$ flow. In the $m=2$ drift-Alfvén wave the ion fluid is flowing in two pairs of counterrotating vortices around the potential hills and valleys of the wave. As the entire mode structure rotates, the direction of the u_R components oscillates in the imaged plasma [compare Figs. 3(a) and 3(b) with 3(c)].

Despite the agreement on the flow pattern between the PLIF measured field and the drift approximation, the magnitudes of the calculated velocities are on average an order of magnitude larger than those actually measured (see Fig. 5). The discrepancies in the overall magnitude are not within the $\sim 50\%$ error inherent in calculating the drift approximation prediction. Attempts to include polarization terms, the convective derivative and the Alfvén character of the wave do not resolve this discrepancy in magnitudes. The drift approximation simply fails to predict the correct magnitude of the ion fluid flow. Although stochasticity accounts for the high mean ion temperature [4], there is no theory that incorporates collective effects due to stochastic dynamics that would explain these results.

A possible mechanism for the observed reduction in the ion fluid response is averaging of the wave electric field due to stochastic ion orbits. Conventional finite Larmor radius (CFLR) theory [12] predicts that a similar averaging effect reduces the fluid velocity in a plane wave by a factor of $e^{-s}I_0(s)$ where $s = k_\perp^2 r_L^2$. However, CFLR theory is not strictly applicable here since CFLR assumes both linearization of the Vlasov equation and integration along unperturbed orbits whereas the drift wave amplitude here is large enough to invalidate linearization and furthermore stochastic ion orbits are very different from unperturbed orbits. Nevertheless, CFLR should give a reasonable estimate of the reduction of the fluid velocity because we expect that the wave phase averaging due to large orbits should be relatively insensitive to the exact nature of the orbits. Using $k_\perp = 27\ \mathrm{m}^{-1}$ and $r_L = (\kappa T_i/m_i)^{1/2}/\omega_{ci}$ with $T_i = 6$ eV gives $s = 2.4$ for our parameters yielding a CFLR reduction factor of 0.27 which is the correct order of magnitude to explain our observations.

In summary, the first plasma PLIF diagnostic has been used to study the ion-fluid velocity in coherent drift waves above the stochastic threshold in Caltech's Encore tokamak. The PLIF measured ion-fluid velocity components in the drift wave agree qualitatively with the flow pattern predicted by the fluid drift approximation despite stochastic dynamics of particles in the bulk of the distribution. However, the measured magnitude of the fluid velocity is an order of magnitude smaller than predicted by fluid theory. We believe this discrepancy is similar to the finite Larmor radius effect in that the phase seen by the ions is averaged as the ions trace their large stochastic orbits, resulting in a reduced macroscopic fluid velocity.

We wish to thank Frank Cosso for assistance with electronics. This work was supported by NSF Grant No. PHY-9114146.

*Present address: AT&T Bell Laboratories, Murray Hill, NJ 07974.

†Permanent address: University of Colorado, Boulder, CO 80309.

[1] B. B. Kadomtsev, Nucl. Fusion **31**, 1301 (1991); B. Weyssow, J. H. Miguich, and R. Balescu, Plasma Phys. Controlled Fusion **33**, 763 (1991); J. R. Cary, D. F. Escande, and A. D. Verga, Phys. Rev. Lett. **65**, 3132 (1990); Geophys. Res. Lett. **18**, 1573ff. (1991), twenty papers on stochasticity in space plasmas.

[2] E. D. Fredrickson and P. M. Bellan, Phys. Fluids **28**, 1866 (1985).

[3] F. Skiff, F. Anderegg, T. N. Good, P. J. Paris, M. Q. Tran, N. Rynn, and R. A. Stern, Phys. Rev. Lett. **61**, 2034 (1988); F. Skiff, F. Anderegg, and M. Q. Tran, Phys. Rev. Lett. **58**, 1430 (1988).

[4] J. M. McChesney, R. A. Stern, and P. M. Bellan, Phys. Rev. Lett. **59**, 1436 (1987); J. M. McChesney, P. M. Bellan, and R. A. Stern, Phys. Fluids B **3**, 3363 (1991).

[5] R. J. Groebner, K. H. Burrell, and R. P. Seraydarian, Phys. Rev. Lett. **64**, 3015 (1990); K. Ida, S. Hidekuma, Y. Miura, T. Fujita, M. Mori, K. Hoshimo, N. Suzuki, T. Yamauchi, and JFT-2M Group, Phys. Rev. Lett. **65**, 1364 (1990).

[6] T. Peyser and G. C. Goldenbaum, Phys. Rev. Lett. **61**, 955 (1988).

[7] F. Anderegg, R. A. Stern, F. Skiff, E. A. Hammel, M. Q. Tran, P. J. Paris, and P. Kohler, Phys. Rev. Lett. **57**, 329 (1986).

[8] R. A. Stern, D. L. Correll, H. Bohmer, and N. Rynn, Phys. Rev. Lett. **37**, 833 (1976); R. A. Stern, D. N. Hill, and N. Rynn, Phys. Rev. Lett. **47**, 792 (1981); R. McWilliams and D. Sheehan, Phys. Rev. Lett. **56**, 2485 (1986); F. Skiff and F. Anderegg, Phys. Rev. Lett. **59**, 896 (1987).

[9] G. Kychakoff, R. D. Howe, R. K. Hanson, and J. C. McDaniel, Appl. Opt. **21**, 3225 (1982).

[10] G. Norlén, Phys. Scr. **8**, 249 (1973).

[11] I. H. Hutchinson, *Principles of Plasma Diagnostics* (Cambridge Univ. Press, New York, 1987).

[12] M. N. Rosenbluth, N. A. Krall, and N. Rostoker, Nucl. Fusion Suppl. Part **1**, 143 (1962).

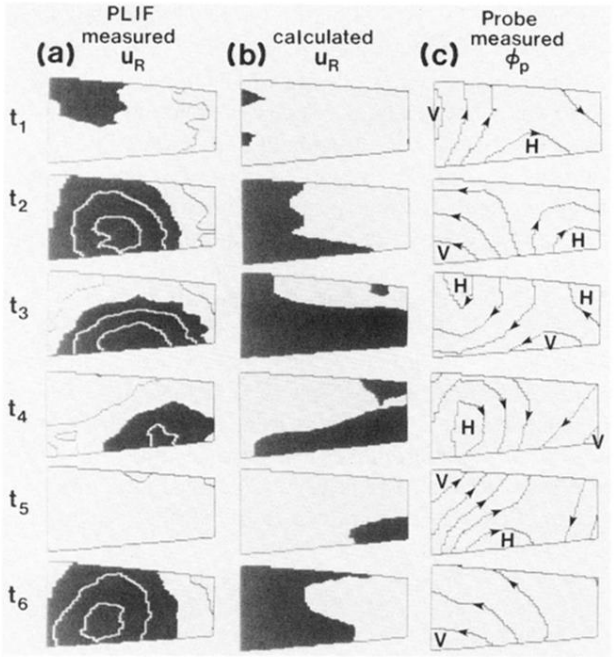

FIG. 3. (a) PLIF measured u_R field [full scale $\pm 1.1\times10^5$ cm/s, 2.8×10^4 (cm/s)/contour]. (b) u_R field calculated from probe and PLIF data in the drift approximation. Black (white) indicates u_R velocities to the left (right). (c) Langmuir probe measured $\tilde{\phi}_p$ (2 V/contour). Arrows on the equipotentials indicate the direction of $\mathbf{E}\times\mathbf{B}$ drifts around potential hills (H) and potential valleys (V). $\mathbf{B}$ points out of the page so that the electron diamagnetic rotation is counterclockwise. Times ($\Delta t = 40$ μs) correspond to those marked in Fig. 2. See Fig. 1 for correct spatial scales.

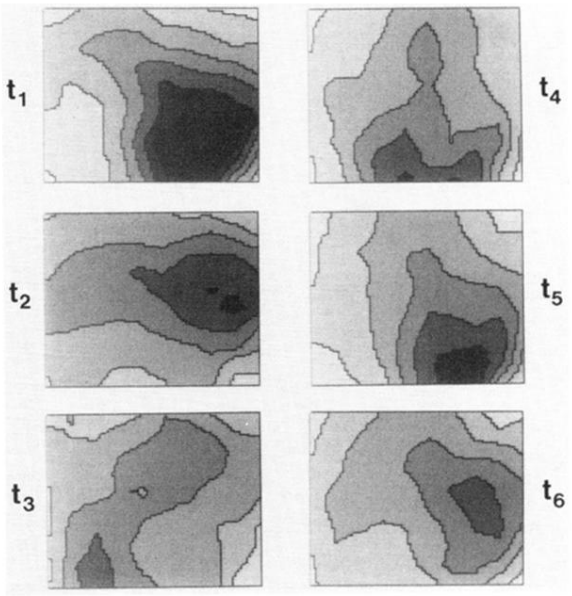

FIG. 4. Plasma density in a poloidal cross section showing dominant $m=2$ mode structure (peak density 3×10^{12} cm^{-3}, $\sim5\times10^{11}$ cm^{-3}/contour). **B** points out of the page so that the electron diamagnetic rotation is counterclockwise. Times ($\Delta t=40$ μs) correspond to those marked in Fig. 2. See Fig. 1 for correct spatial scales.